



THE UNIVERSITY *of* EDINBURGH

Edinburgh Research Explorer

## Redox Potential Dependence of Peptide Structure Studied Using Surface Enhanced Raman Spectroscopy

**Citation for published version:**

Ochsenkuehn, MA, Borek, JA, Phelps, R & Campbell, CJ 2011, 'Redox Potential Dependence of Peptide Structure Studied Using Surface Enhanced Raman Spectroscopy', *Nano Letters*, vol. 11, no. 7, pp. 2684-2688. <https://doi.org/10.1021/nl200885p>

**Digital Object Identifier (DOI):**

[10.1021/nl200885p](https://doi.org/10.1021/nl200885p)

**Link:**

[Link to publication record in Edinburgh Research Explorer](#)

**Document Version:**

Peer reviewed version

**Published In:**

Nano Letters

**Publisher Rights Statement:**

Copyright © 2011 by the American Chemical Society; all rights reserved.

**General rights**

Copyright for the publications made accessible via the Edinburgh Research Explorer is retained by the author(s) and / or other copyright owners and it is a condition of accessing these publications that users recognise and abide by the legal requirements associated with these rights.

**Take down policy**

The University of Edinburgh has made every reasonable effort to ensure that Edinburgh Research Explorer content complies with UK legislation. If you believe that the public display of this file breaches copyright please contact [openaccess@ed.ac.uk](mailto:openaccess@ed.ac.uk) providing details, and we will remove access to the work immediately and investigate your claim.



This document is the Accepted Manuscript version of a Published Work that appeared in final form in *Nano Letters*, copyright © American Chemical Society after peer review and technical editing by the publisher. To access the final edited and published work see <http://dx.doi.org/10.1021/nl200885p>

Cite as:

Ochsenkühn, M. A., Borek, J. A., Phelps, R., & Campbell, C. J. (2011). Redox Potential Dependence of Peptide Structure Studied Using Surface Enhanced Raman Spectroscopy. *Nano Letters*, 11(7), 2684-2688.

Manuscript received: 17/03/2011; Accepted: 21/05/2011; Article published: 07/06/2011

## Redox Potential Dependence of Peptide Structure Studied Using Surface Enhanced Raman Spectroscopy\*\*

Michael A. Ochsenkühn,<sup>1</sup> Joanna A. Borek,<sup>2</sup> Richard Phelps<sup>3</sup>  
and Colin J. Campbell<sup>1,4,\*</sup>

<sup>[1]</sup>EaStCHEM, School of Chemistry, Joseph Black Building, University of Edinburgh, West Mains Road, Edinburgh, EH9 3JJ, UK.

<sup>[2]</sup>Physikalisch-chemisches Institut, Universität Zürich, Winterthurerstrasse 190, CH-8057 Zürich, Switzerland.

<sup>[3]</sup>QMRI, University of Edinburgh, 49 Little France Crescent, Edinburgh, EH16 4SB, U.K.

<sup>[4]</sup>Division of Pathway Medicine, Chancellors Building, University of Edinburgh, 49 Little France Crescent, Edinburgh, EH16 4SB, U.K.

<sup>[\*]</sup>Corresponding authors; e-mail: M.A.O. [mochsenk@ed.ac.uk](mailto:mochsenk@ed.ac.uk); C.J.C. [colin.campbell@ed.ac.uk](mailto:colin.campbell@ed.ac.uk), tel: +44 (0)131 242 647; fax: +44 (0)131 242 6244

<sup>[\*\*]</sup>We would like to thank EastCHEM and the School of Chemistry of UoE for funding. We are also very grateful to Professor E. Campbell and her workgroup for the opportunity to work on Raman and AFM instruments and for fruitful advice.

### Supporting information:

Additional information available free of charge via the internet at <http://pubs.acs.org/>

### Keywords:

SERS; nanoshell; peptide; redox; Goodpasture's; proteolysis

## Abstract

We describe a novel surface enhanced Raman spectroscopy (SERS) sensing approach utilizing Auroshell™ gold Nanoshells and demonstrate its application to analysis of critical redox-potential dependent changes in antigen structure that are implicated in the initiation of a human autoimmune disease. In Goodpasture's disease, an autoimmune reaction is thought to arise from incomplete proteolysis of the autoantigen,  $\alpha 3(\text{IV})\text{NC1}(67-85)$  by proteases including Cathepsin D. We have used SERS to study conformational changes in the antigen that correlate with its oxidation state and to show that the antigen must be in the reduced state in order to undergo proteolysis. Our approach determined that an intracellular redox-potential of  $\sim 200$  mV was sufficient for reduction, pre-requisite for productive processing, of the intramolecular disulfide bond within the antigenic fragment  $\alpha 3(\text{IV})\text{NC1}_{67-85}$ . Moreover we demonstrate that interaction of the antigenic fragment with Cathepsin D, is vastly facilitated by reduction of this disulfide bond and that the peptide bonds subsequently cleaved by Cathepsin D can be identified by consultation of a SERS library of short synthetic peptides.

## Introduction

The investigation of a wide range of diseases is currently limited by a lack of suitably specific and versatile bioanalytical tools. Recently, Surface enhanced Raman spectroscopy (SERS) has been used for a large variety of bioanalytical applications, including single molecule studies,<sup>1</sup> oligonucleotide sequencing<sup>2</sup> and for probing peptide and protein structure.<sup>3-6</sup> SERS can also be used for imaging the intracellular environment of cells and has been demonstrated using a variety of noble metal particles which are readily delivered to mammalian cells.<sup>4,7,8</sup> Gold nanoshells (NS) are engineered nanoparticles and we have recently demonstrated that their characteristics make them ideal for intracellular SERS studies.<sup>5,9-13</sup> We have also recently demonstrated that NS are ideal substrates for the measurement of conformational changes in biomolecules and that this property can be used for direct measurement of biomolecular interactions.<sup>14</sup>

Goodpasture's Disease is a rare autoimmune condition of the kidneys and lungs in which there is a B-cell and T-cell response to a non-collagenous domain of the alpha-3 chain of type IV collagen ( $\alpha 3(\text{IV})\text{NC1}$ ). It is thought that in the course of usual  $\alpha 3(\text{IV})\text{NC1}$  processing within the antigen presenting cells of healthy individuals, certain  $\alpha 3(\text{IV})\text{NC1}$  peptides are not processed for presentation to T cells because of their consistent destruction in the course of processing (destructive processing).<sup>15</sup> As a result, T-cells specific for the destroyed self-peptides might avoid mechanisms that usually control the activation of potentially autoreactive T cells. In support of this hypothesis, T-cells specific for certain  $\alpha 3(\text{IV})\text{NC1}$  peptides (epitopes) can be detected in healthy individuals as well as patients

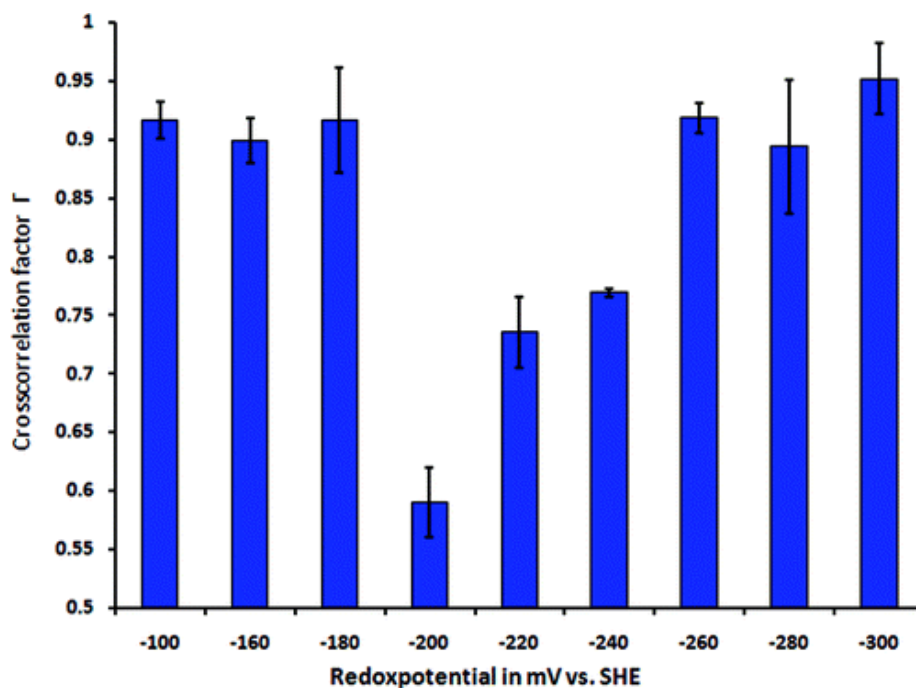
with Goodpasture's disease, and at least one of the major T cell epitopes,  $\alpha 3(\text{IV})\text{NC1}_{67-85}$ , has been shown to be consistently destroyed in the course of  $\alpha 3(\text{IV})\text{NC1}$  processing by B cell lysosomes:  $\alpha 3(\text{IV})\text{NC1}$  processing was initiated by an 'unlocking' step that required the  $3(\text{IV})\text{NC1}_{67-85}$  peptide first undergo reduction of a disulfide bridge that holds it in a hairpin-like conformation, and second be cleaved by an aspartate protease, probably Cathepsin D.<sup>16,17</sup> This finding suggests that the redox environment during  $3(\text{IV})\text{NC1}$  processing may be important in determining whether processing proceeds as described with destruction of  $\alpha 3(\text{IV})\text{NC1}_{67-85}$ , or some other route in which  $\alpha 33(\text{IV})\text{NC1}_{67-85}$  is preserved and autoreactive T cells are activated. It is important to measure the standard redox potential of the disulfide bond of the peptide.

In this work we sought to use SERS to investigate the conformational changes undergone by a fragment of the Goodpasture's antigen in response to different redox potentials. By correlating conformational heterogeneity with potential we were able to estimate the standard potential for the dithiol bond. Furthermore we have used SERS to study the interaction between the peptide and Cathepsin D (its cognate protease) and have investigated the redox dependent digestion of the peptide. We have found that the potentials required for reduction of the dithiol bond correlate extremely well with those required for digestion. Furthermore, we have used SERS to estimate the site of digestion of the peptide. Finally, we have used SERS to detect digestion and protein binding in live cells.

## Results and discussion

In order to measure SERS spectra from the peptide, we assembled gold nanoshell aggregates using an established protocol,<sup>14</sup> and attached the peptide to the gold via a free thiol at its C-terminus. The peptide solution (Clonestar Peptide Services, CZ), 1 mM peptide in pH 7.0 Tris-HCl buffer, 100 mM NaCl and 10 mM  $\text{MgCl}_2$ ) was incubated on the gold aggregates for three days prior to washing, unreacted surface sites were then blocked by incubation with mercaptohexanol (10 mM, 0.5 h) followed by washing in pH 7.0 Tris-HCl buffer, 100 mM NaCl and 10 mM  $\text{MgCl}_2$  (supporting information). We measured SERS spectra at a range of defined potentials at pH 3.2, where the protease is known to possess optimal activity.<sup>18</sup> The potential was defined through control of the relative amounts of oxidized and reduced glutathione in accordance with the Nernst Equation.<sup>19</sup>

All Raman spectra were collected using a Renishaw InVia Raman system with a 785 nm diode laser illuminating the sample with a power of 30 mW through a 50x Leica water objective (NA 0.8) on a heat controlled stage at 25 °C and 37 °C.



**Scheme 1.** Diagonal cross-correlation factors  $\Gamma$  calculated with Pearson function correlating 25 spectra at GSH/GSSG adjusted redoxpotentials from -100 mV to -300 mV. Values close to 1 describe conformational stability, and decreasing  $\Gamma$  values depict a dynamic conformational change. The dip at -200 mV suggests the dynamic breaking and formation of the internal disulfide bond of AS35. The error bars describe a single standard deviation over 3 independent experiments.

At oxidizing potentials we expect the peptide attached to the nanoshells to be a homogeneous population of stably oxidized molecules. As the potential becomes progressively reducing, an increasing proportion of the population should become reduced - at the standard potential half of the population will be reduced and half oxidized and these two sub-populations will be in a dynamic equilibrium. At this potential we therefore expect to see the greatest degree of heterogeneity in the sample and also the greatest degree of dynamic switching between conformers. As the potential is then taken to more strongly reducing conditions, the population again becomes progressively more uniformly reduced and homogeneous. In order to look for potential dependent conformational changes of the type described above, we carried out cross-correlation analysis of 25 individual SERS spectra collected at the same potential. Cross-correlation was calculated using the Pearson cross-correlation factor, standardly used for SERS reproducibility determination,<sup>5</sup> values from 0-1 show the quality of spectral agreement. By carrying out this analysis we expect to be able to measure the degree of heterogeneity of the population and also the degree of dynamism within the population - a high cross-correlation should indicate a stable homogeneous population and a low cross-correlation should indicate a dynamic heterogeneous population.

When we analyzed the results of these experiments ( Scheme 1) we indeed found a high crosscorrelation in oxidizing conditions with a pronounced dip at approximately -200 mV vs NHE, which is followed by a gradual increase as we moved towards increasingly reducing conditions. At -200 mV the peptide is in a dynamic equilibrium between the oxidised (closed) and reduced (linear). The more we increase the potential towards more oxidizing values the more we push the equilibrium to a stable linearized conformation. These data confirm that at the most oxidizing and reducing potentials tested, there is a static, homogeneous population of molecules and that between these extremes we observe a heterogeneous, dynamic population - on this basis we can estimate the standard (breaking) potential for the peptide under these conditions to be approximately -200 mV vs NHE. While these data provide an approximate value for the standard reduction potential of the peptide, it raises the question - how well do these conformational changes correlate with the ability of the protease Cathepsin D to recognize and to digest the peptide<sup>16</sup> In order to investigate this we measured the SERS spectrum of the peptide bound on NS as before, during and after incubation with Cathepsin D at -250mV. Scheme 2b shows these spectra: before digestion the spectrum exhibits strong sharp peaks; on incubation with Cathepsin D the spectrum maintains its features and actually gains some new sharp, intense peaks; after 30 minutes while the spectrum still contains some defined spectral features its intensity is greatly reduced and the area under the spectrum is reduced ~70%. When the activity of Cathepsin D is blocked by co-incubation with pepstatin A (a known inhibitor) we find no increase in signal due to Cathepsin binding and no decrease in intensity as a result of digestion - this confirms that the spectral changes observed are caused by interaction between the peptide and Cathepsin D. We attribute increase in signal as a result of Cathepsin D binding to conformational changes in the peptide or contributions to the spectrum from vibrational modes of the protease. While further investigation is certainly required to confirm the origin of these features, we and others have previously demonstrated that conformational changes in aptamer structure as a result of protein binding cause changes in the intensity and position of peaks in its spectrum.<sup>14</sup> Furthermore, several of the new peaks which arise during incubation with Cathepsin D correlate well with vibrational modes of amino acids at the entrance to the Cathepsin D binding site which are not represented in the peptide (Assignment of the extremely strong feature at 1258 cm<sup>-1</sup> and strong and sharp features at 670 cm<sup>-1</sup>, 854 cm<sup>-1</sup>, 1002 cm<sup>-1</sup> or 1425 cm<sup>-1</sup> in the "bound" correlates well with the spectra of Tyr and of Phe.<sup>5,20,21</sup>). Importantly, the quantifiable decrease in spectral intensity (measured as the difference between the integral under the curve before and after digestion) is an ideal way in which to compare the extent of digestion at different potentials. Scheme 2c shows the change in spectral area caused by digestion as a function of potential and clearly shows that there is only a measurable change in intensity as a result of digestion at potentials more negative than -200 mV vs NHE with the extent of digestion increasing towards more reducing conditions. When the digestion was carried out at -300 mV in the presence of pepstatin (an inhibitor of Cathepsin D) there was no measurable change in spectral intensity. The results of digestion at different potentials agree with

those measured on the basis of population heterogeneity in (Scheme 1) and confirm that the increase in extent of digestion correlates well with the transition from oxidized to reduced peptide.

While the above data gives quantitative information about the potential at which peptide cleavage occurs, it does not give any information about the site of cleavage or the chemical composition of the residual peptide on the nanoshell surface. While it is clear that the Raman spectrum of the residual peptide on the nanoshell contains well defined features it is not trivial to either predict their assignments or to assign them by comparison to existing literature values. Therefore, in order to try to understand the spectrum of the residual peptide better, we first measured spectra of each of its individual amino acids. We measured these spectra by attaching homo-trimers of each amino acid to the surface of the nanoshells so that each molecule could experience an element of the conformational freedom available which would be available to it in the peptide. Using this library of spectra we constructed model spectra of each of the possible residual cleavage products by simply adding together the spectra of the component amino-acids. Each of these "model" spectra were then compared to the spectrum of the post-digest residual peptide using a Spearman correlation. In order to aid comparison of spectra on the basis of peak position, the first derivative of the spectra were calculated after averaging and background subtraction, and correlation was calculated using the correlation coefficient function in Equation (1). The advantage in the use of the Spearman rank correlation factor lies in its ability to compare curved features better, with significant values of 0.01 and the possibility to determine anti-correlation.

(1)

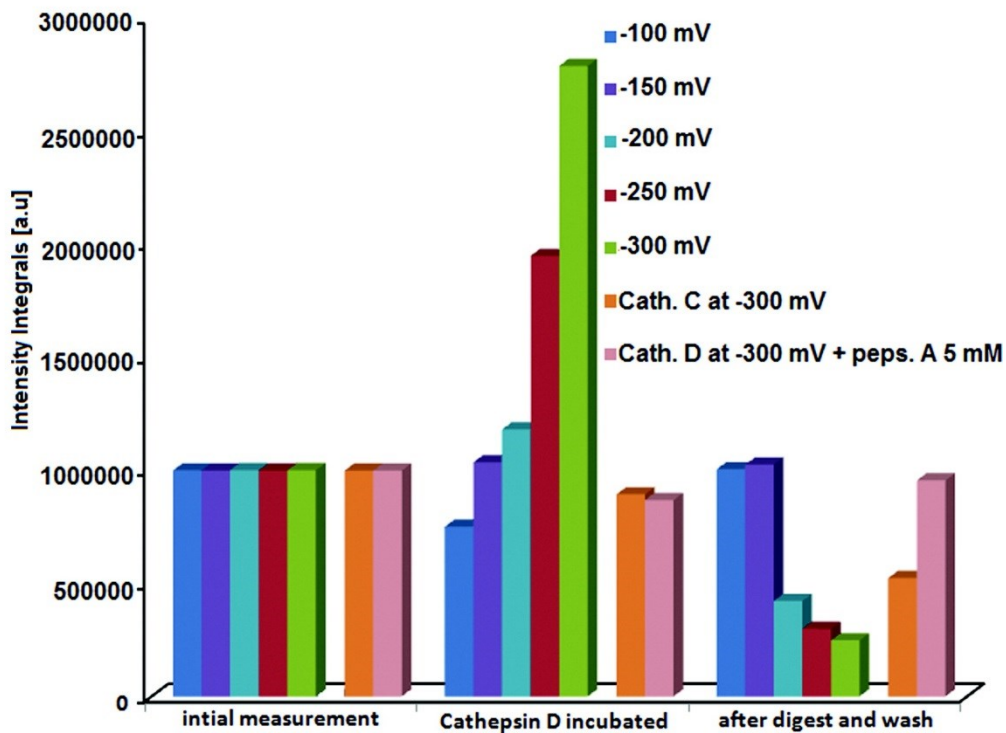
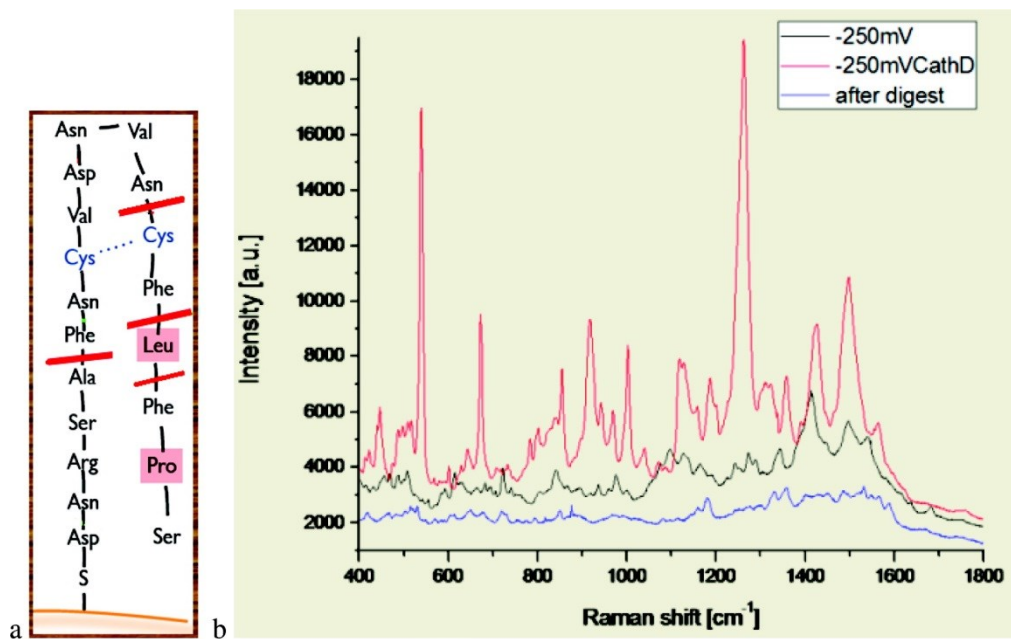
$$\rho = 1 - \frac{6\sum d_i^2}{n(n^2 - 1)}$$

$\rho$  Spearman Rank correlation

$d_i$  difference between the ranks of corresponding values ( $y_i - x_i$ )

$n$  number of values in each data set

Comparison of the post-digest residual peptide with all the possible model spectra gives a gradual increase in correlation up until the first Phe as seen in Scheme 3. After this point there is a gradual loss in correlation as the model peptide grows in length. This data suggests that the closest site of peptide cleavage to the surface of the particle is between Phe and Asn and this finding correlates well with the known restriction sites for Cathepsin D digestion of this peptide.<sup>16</sup> When the model spectra are compared with the spectrum of the peptide which was treated with Cathepsin D at -100 mV, where there was no loss in spectral intensity there is a gradual increase in correlation until the ninth position where the bend in the peptide could be predicted with slight decrease in the correlation factor after this point and might be caused by some digestion at the N-terminal.

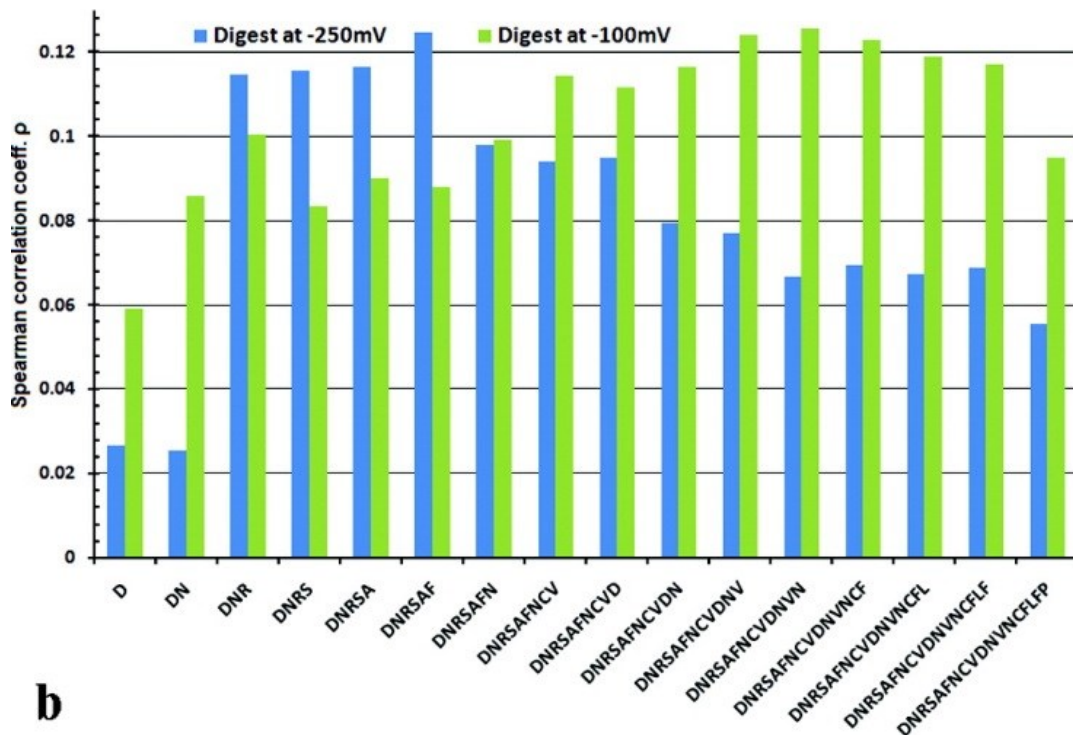
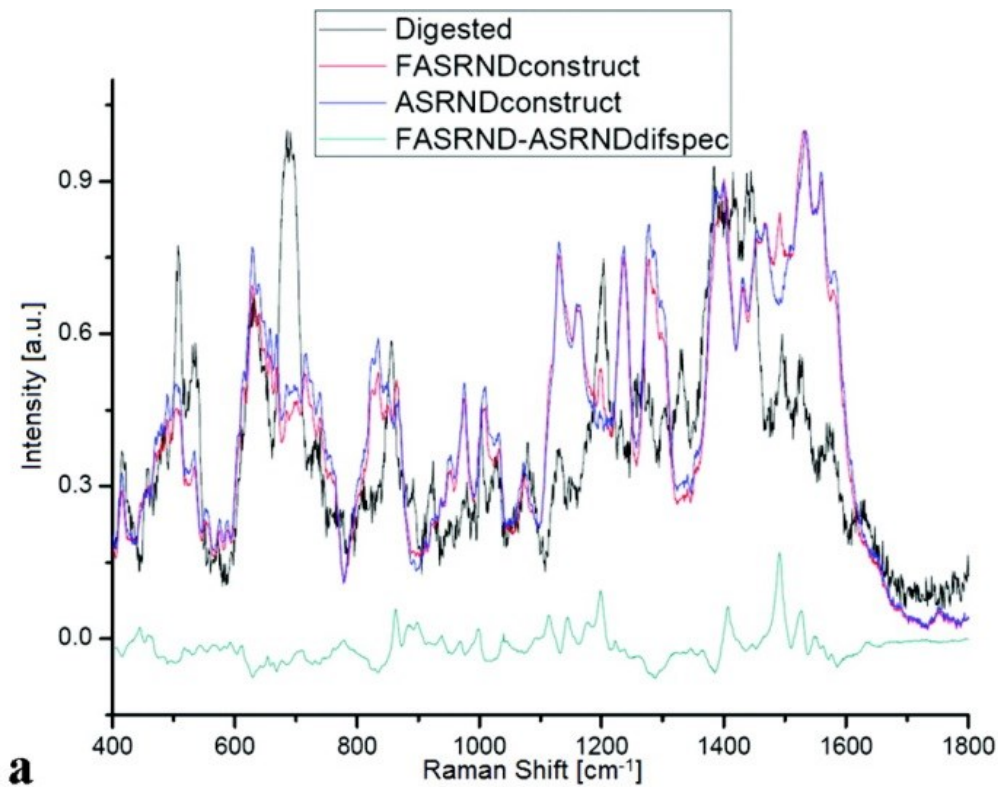


**Scheme 2.** a) Sketch showing the closed form of the peptide bound with its C-terminus (Asp) to the NS surface with Cathepsin D restriction sites in red. b) Average of 25 spectra of digestion experiment with Cathepsin D at -250 mV. Shown spectra are after preincubation with buffer at -250 mV (black), directly after the incubation with Cathepsin D (red) and after incubation, denaturation and wash of the sensor (blue). c) Integrals of digestion experiments at redoxpotentials of -100, -250, -300 mV and control experiments with non-AS35 specific protease Cathepsin C and pepstatin inhibited Cathepsin D at -300 mV, comparing before, during and after the incubation with Cathepsin.



Scheme 3a compares the experimentally measured spectrum of the digested peptide, at -250 mV with the Raman model obtained from the AA-library for two possible fragments Ala-Ser-Arg-Asn-Asp (ASRND) and Phe-Ala-Ser-Arg-Asn-Asp (FASRND). We have focussed on these fragments because the FASRND bond is the shortest residual peptide predicted on the basis of known restriction sites and should correlate better than ASRND.<sup>16</sup> The first notable observation here is that while the spectra of ASRND and FASRND show many similarities with the Raman features of the measured spectrum there are significant differences as between 440 cm<sup>-1</sup> and 560 cm<sup>-1</sup> or in the range between 600 cm<sup>-1</sup> and 700 cm<sup>-1</sup> where peak positions and intensities match between the experimental and the model data. Furthermore when comparing the spectra of the model peptides with the experimental it is clear that vibrational modes from phenylalanine are represented in the experimental spectrum. Examples for this are the features at 1220 cm<sup>-1</sup> and 1540 cm<sup>-1</sup>, which can be assigned to the aromatic ring stretches of the Phe as shown in Scheme 3a.<sup>20,22</sup> A comparison between correlation coefficients the sum of the model differential AA-spectra of the protease restriction experiments at -250 mV and -100 mV vs NHE gives further indication as shown in Scheme 3b. At -250 mV the G value rises to a maximum at the predicted restriction site with an abrupt decrease after the corresponding Phe. Furthermore, at -100 mV no similar feature can be found. That means that the construction of AA-chain model spectra can be used to determine residuals peptide fragments by SER spectroscopy.

**(turn to next page →)**



**Scheme 3.** a) Spectral comparison between constructed peptides ASRND and FASRND and the spectrum acquired after digest at -250 mV, including the difference spectrum between the models FASRND-ASRND. b) Spearman cross correlation comparison between constructed peptides of AS35 up to Proline and the same digestion experiment.

In summary, we have shown that SERS can be used to investigate the electrochemistry of a peptide. Further, we have shown that the pseudo-standard reduction potential of the peptide correlates with the reactivity of this peptide with its cognate protease. Finally we have shown that SERS can be used to give information on the products of digestion. These findings open exciting possibilities for investigating the redox control of protein/protein interactions and the measurement of conformational states of biomolecules.

## References

- [1] Nie, S.; Emory, S. R. *Science* 1997, 275, **1102–1106**.
- [2] MacAskill, A.; Crawford, D.; Duncan Graham, D.; Faulds, K. *Anal. Chem.* 2009, 81, **8134–8140**.
- [3] Feng, M.; Hiroyasu Tachikawa, H. *Journal of the American Chemical Society* 2008, 130, **7443–7448**.
- [4] Bale, S.; Kwon, S.; Shah, D.; Banerjee, A.; Dordick, J.; Kane, R. *ACS Nano* 2010, 4, **1493–1500**.
- [5] Wei, F.; Zhang, D.; Halas, N.; Hartgerink, J. *Journal of Physical Chemistry B* 2008, 112, **9158–9164**.
- [6] Feng, M.; Tachikawa, H. *Journal of the American Chemical Society* 2008, 130, **7443–7448**.
- [7] Kneipp, J.; Kneipp, H.; Wittig, B.; Kneipp, K. *Nano Letters* 2007, 7, **2819–2823**.
- [8] Kneipp, J.; Kneipp, H.; McLaughlin, M.; Brown, D.; Kneipp, K. *Nano Letters* 2006, 6, **2225–2231**.
- [9] Brinson, B.; Lassiter, J.; Levin, C.; Bardhan, R.; Mirin, N.; Halas, N. *Langmuir* 2008, 24, **14166–14171**.
- [10] Ochsenkühn, M.; Jess, P.; Stoquert, H.; Dholakia, K.; Campbell, C. *ACS Nano* 2009, 3, **3613–3621**.
- [11] Chowhudry, M.; Campbell, C.; Theofanidou, E.; Seung Joon, L.; Baldwin, G., A. Sing; Yeh, A.; Crain, J.; Ghazal, P.; Cote, G. *Progress in biomedical optics and imaging* 2006, 7, **609905.1–609905.8**.
- [12] Barhoumi, A.; Zhang, D.; Tam, F.; Halas, N. *Journal of the American Chemical Society* 2008, 130, **5523–5529**.
- [13] Barhoumi, A.; Zhang, D.; Halas, N. *Journal of the American Chemical Society* 2008, 130, **14040–14041**.
- [14] Ochsenkühn, M. A.; Campbell, C. *Chemical Communications* 2010, 46, **2799**.
- [15] Manoury, B.; Mazzeo, D.; Fugger, L.; Viner, N.; Ponsford, M.; Streeter, H. *Nature Immunology* 2002, 3, **169–174**.

- [16] Zou, J.; Hannier, S.; Cairns, L.; Baker, R.; Rees, A.; Turner, A.; Phelps, R. *Journal of the American Nephrological Society* 2008, 19, **396–404**.
- [17] Zou, J.; Henderson, L.; Thomas, V.; Swan, P.; Turner, A.; Phelps, R. *Journal of the American Nephrological Society* 2007, 18, **771–779**.
- [18] A.J., B. *Biochemical Journal* 1970, 117, **601–607**.
- [19] Schafer, F.; Buettner, G. *Free Radical Biology & Medicine* 2001, 30, **1191–1212**.
- (20) Ota, F.; Higuchi, S.; Gohshi, Y.; Furuya, K.; Ban, M.; Kyoto, M. *Journal of Raman spectroscopy* 1997, 28, **849–854**.
- [21] Jenkins, A.; Larsen, R.; Williams, T. *Spectrochimica Acta Part A* 2005, 61, **1585–1594**.
- [22] De Gelder, J.; De Gussem, K.; Vandenabeele, P.; Luc Moens, L. *Journal of Raman spectroscopy* 2007, **38**.